Zhou et al. Biochar (2024) 6:55
https://doi.org/10.1007/s42773-024-00349-8

Biochar

ORIGINAL RESEARCH

Open Access

# Synergistic effect between biochar and sulfidized nano-sized zero-valent iron enhanced cadmium immobilization in a contaminated paddy soil

Yu Zhou[1], Lu Lv[1], Zhi Yu[2], Jian Zhang[1*], Bing Wang[3], Ruidong Yang[3], Miao Chen[3], Pan Wu[1] and Shengsen Wang[4*]

## Abstract

Biochar-based sulfidized nano-sized zero-valent iron (SNZVI/BC) can effectively immobilize cadmium (Cd) in contaminated paddy soils. However, the synergistic effects between biochar and SNZVI on Cd immobilization, as well as the underlying mechanisms remain unclear. Herein, a soil microcosm incubation experiment was performed to investigate the immobilization performance of SNZVI/BC towards Cd in the contaminated paddy soil. Results indicated that the addition of SNZVI/BC at a dosage of 3% significantly lessened the concentration of available Cd in the contaminated soil from 14.9 (without addition) to 9.9 mg $kg^{-1}$ with an immobilization efficiency of 33.3%, indicating a synergistic effect. The sequential extraction results indicated that the proportion of the residual Cd in the contaminated soil increased from 8.1 to 10.3%, manifesting the transformation of the unstable Cd fractions to the steadier specie after application of SNZVI/BC. Also, the addition of SNZVI/BC increased soil pH, organic matter, and dissolved organic carbon, which significantly altered the bacterial community in the soil, enriching the relative abundances of functional microbes (e.g., *Bacillus*, *Clostridium*, and *Desulfosporosinus*). These functional microorganisms further facilitated the generation of ammonium, nitrate, and ferrous iron in the contaminated paddy soil, enhancing nutrients' availability. The direct interaction between SNZVI/BC and $Cd^{2+}$, the altered soil physicochemical properties, and the responded bacterial community played important roles in Cd immobilization in the contaminated soil. Overall, the biochar-based SNZVI is a promising candidate for the effective immobilization of Cd and the improvement of nutrients' availability in the contaminated paddy soil.

## Highlights

- Biochar-based sulfidized nano-sized zero-valent iron (SNZVI/BC) synergistically immobilized Cd in the contaminated soil.
- SNZVI/BC effectively enhanced nutrients' availability in the contaminated soil.
- Nitrate-, Iron-, and sulfate-reducing bacteria were enriched in the SNZVI/BC-treated soil.

Handling editor: Xing Yang.

*Correspondence:
Jian Zhang
jzhang21@gzu.edu.cn
Shengsen Wang
wangss@yzu.edu.cn
Full list of author information is available at the end of the article

- Precipitation and complexation played an important role in the immobilization of Cd.

**Keywords** Biochar, Potentially toxic element, Soil remediation, Microbial response, Sulfidized nano-sized zero-valent iron

**Graphical Abstract**

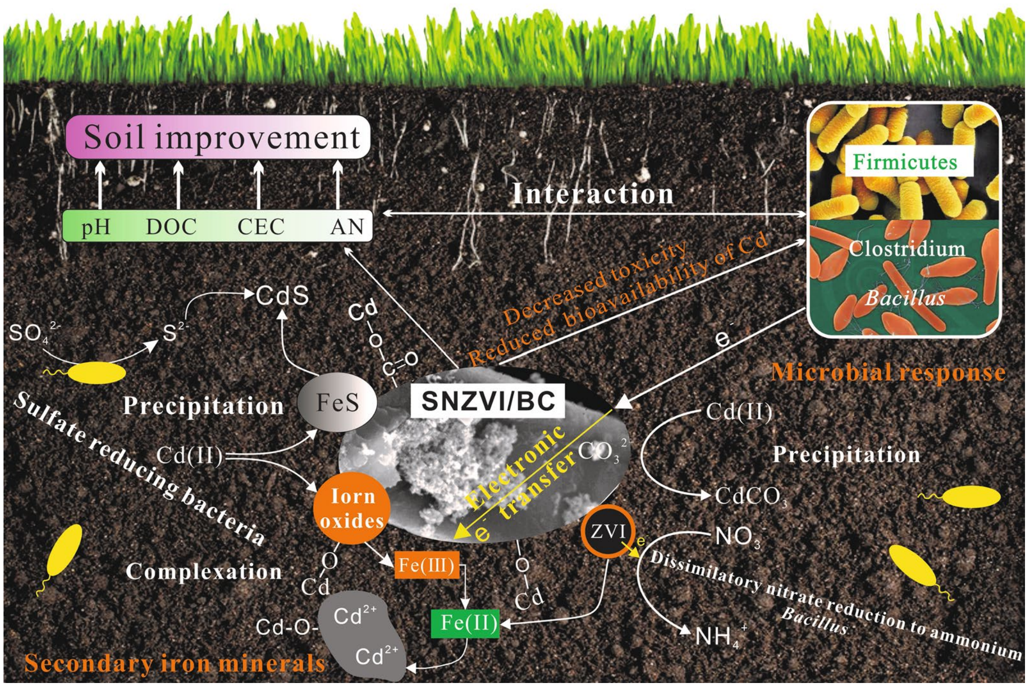


## 1 Introduction

Cadmium (Cd) is one of the most common potentially toxic elements in arable soils. As a carcinogenic metal, Cd is highly toxic and can be transformed to human body through the food chain (Zhang et al. 2023e), which poses a potential risk to human health. Therefore, Cd pollution in soils has attracted much attention from the public. Moreover, it is also urgent to develop some feasible technologies to remediate Cd-contaminated arable soils, especially to accomplish the safe use goal of Cd-contaminated paddy soils (Xue et al. 2023). At present, remediation technologies for Cd-contaminated soils mainly include physical remediation, chemical remediation, biological remediation, and combined remediation (Zhang et al. 2021b). No matter which technology, the main principle is to either remove Cd or immobilize it. However, compared with the methods of removing Cd (e.g., electrokinetic remediation, chemical leaching, and hyperaccumulator extraction), chemical immobilization has shown excellent remediation effects (Zhang et al. 2023d), such as simple technical difficulty (Kong et al. 2023a, b), low economic cost, and high immobilization effectiveness. Therefore, this technology was widely used to remediate Cd-contaminated soils (Yang et al. 2023).

Biochar (BC) has been widely used in the immobilization of potentially toxic elements in contaminated soils due to the wide source of feedstocks (Loc et al. 2022), large specific surface area (Shenk et al. 2022), abundant oxygen-containing functional groups, high pH value, and high cation exchange capacity. However, the immobilization performance of the raw BC on potentially toxic elements in contaminated soils is usually not satisfactory, and thus it is necessary to modify BC to improve its remediation performance for the contaminated soils. For example, the combination of *Paecilomyces paecilomyces extracts* and biochar can substantially reduce the concentration of available Cd in the surface soils (Guo et al. 2022). Moreover, applications of $NH_4Cl$-modified corn stalk-derived biochar (NBC) and micro-nano nitrogen-doped biochar reduced the concentrations of available

Cd by 1.3 and 1.4 times, respectively, compared to the pristine corn stalk-derived biochar (CBC) treated soil (Chen et al. 2023a).

In recent years, the emerging nanotechnology played an important role in removing pollutants and remediating contaminated soils. For example, nano-sized zero-valent iron (NZVI) owned high adsorption capacity, large specific surface area, excellent reducibility (Yi et al. 2020), low cost, and low toxicity, which made it a proper agent to immobilize potentially toxic elements in contaminated soils (Xu et al. 2021). However, NZVI is easy to aggregate and form chain-like fine particles, thus weakening its reactivity because of lessened active sites. To solve this problem, BC could be used as a supporting material that could not only inhibit the aggregation of NZVI, but also increase the abundance of functional groups, thereby significantly improving the remediation capacity of materials (Yan et al. 2017). Further, a reported study showed that the sulfidized NZVI (SNZVI) had greater potential in remediating Cd-contaminated soils than the pristine NZVI, which is not only because the existence of FeS in its shell can form insoluble cadmium sulfide by reaction with $Cd^{2+}$ (Su et al. 2015), but also sulfurized modification effectively improves the electron transfer efficiency of NZVI. As a result, greater attention has been paid to SNZVI about its application to environmental remediation such as immobilization of potentially toxic elements (Song et al. 2023), 2,4,6-trichlorophenol dechlorination (Wang et al. 2023a), degradation of Acid Red 73 (Ding et al. 2023), and reductive transformation of tetrabromobisphenol A (Gao et al. 2023). To be specific, a proton-buffering montmorillonite-supported SNZVI was successfully prepared and its reduction efficiency toward water-soluble Cr(VI) was greater than 99% (Zhang et al. 2023f). Moreover, rhamnolipid-coated SNZVI was successfully synthesized and used to stabilize water-soluble Pb, Cd, and As in multi-contaminated soils, achieving the immobilization efficiencies of 88.8%, 72%, and 63%, respectively (Song et al. 2023). A further study indicated that the addition of BC, SNZVI, and biochar-based SNZVI significantly lowered the proportion of HOAc-extractable Cd in the contaminated soil after remediation of 49 days, by 15.9%, 25.5%, and 36.1%, respectively, showing a synergistic effect (Xu et al. 2023a). However, up to now the synergistic effect and mechanism between biochar and SNZVI for the enhanced Cd immobilization in the contaminated soil have not been investigated and clarified in depth.

Microbia plays an important role in elemental biogeochemical cycling in soils. The addition of some materials can change the physicochemical properties of potentially toxic element-contaminated soils, and in turn alter soil microbial communities. These responded microbial communities could be conducive to immobilization of potentially toxic elements via microbial adsorption and accumulation (Zhang et al. 2023c). For example, the application of nitrated hydrochar stimulated the abundances of *Proteobacteria* and *Firmicutes* in soils, promoting their proliferation, which played important roles in immobilizing Cd in contaminated soils (Wu et al. 2023a). Moreover, a recent research showed that the addition of SNZVI increased the abundance of *Protobacteria*, while reduced the abundances of *Actinobacteria* and *Firmicute* in the contaminated soil (Liu et al. 2023a). Furthermore, Han et al. (2022) reported that the co-application of *Bacillus* and ferrihydrite could immobilize more Cd as compared to the mono-application of either *Bacillus* or ferrihydrite. Similarly, as an immobilization carrier of microorganism, biochar can facilitate Cd immobilization via promoting the growth of phosphate solubilizing bacteria (Qi et al. 2023). Additionally, biochar and sulfate-reducing bacteria can synergically improve the immobilization of cadmium, lead, and zinc, because biochar can provide attachment sites for sulfate-reducing bacteria, and enhance the reduction efficiency of sulfate and the generation of metal sulfides (Wu et al. 2022; Ke et al. 2023; Si et al. 2023). The addition of SNZVI also increased the abundance of *Gammaproteobacteria* and decreased the abundance of *Bacteroidia* in the soil (Hui et al. 2022). However, to the best of our knowledge, studies about soil microbial response to application of the biochar-based SNZVI remain relatively limited. Moreover, there is also a lack of in-depth understanding of the biogeochemical transformation process of corresponding nutrients in the contaminated soil.

Therefore, the current study aimed to (1) investigate the immobilization performance of biochar-based SNZVI (SNZVI/BC) towards Cd in contaminated paddy soils, (2) elucidate the changes in physicochemical properties, available nutrients, and microbial community in soils, and (3) clarify the immobilization mechanisms of Cd by biochar-based SNZVI in contaminated soils. The current study can provide a deeper insight into the immobilization process of Cd on the biochar-based nano-sized zero-valent iron, as well as the underlying mechanisms in a Cd-contaminated soil.

## 2 Materials and methods

### 2.1 Preparations of BC, SNZVI, SNZVI/BC, and Cd-contaminated soil

First, pinewood sawdust was used as feedstock to fabricate BC in a tube furnace under the limited oxygen condition at 700 °C. A previous study indicated that biochars produced at 700 °C performed better in decreasing the concentration of bioavailable Cd in the sediment (Zhang et al. 2020). SNZVI was synthesized via one-step liquid phase reduction procedure based on the reported literature (Liang et al. 2020). Moreover, the composite SNZVI/BC was fabricated using the same method as SNZVI and keeping the S to Fe molar ratio of 0.75 and the SNZVI to BC mass ratio of 1:2. Further, the original Cd-free soil was collected from Xingren City, Guizhou Province, China. The soil type is ultisol and was formed from the weathering of karstic carbonate rocks. The Cd-spiked contaminated paddy soil was prepared by adding $CdCl_2$ solution (soil:solution = 1:2) to the original soil. The mixture was stirred well, and the contaminated soil was gained after aging for 1 month. The concentration of total Cd in the simulated Cd-contaminated soil was 30 mg $kg^{-1}$. The physicochemical properties of the obtained Cd-contaminated paddy soil used in the present study are shown in Table S1.

### 2.2 Experimental design

Fifty grams of the Cd-contaminated soil were added into polyethylene bottles, and SNZVI, BC, and biochar-based SNZVI were added to the polyethylene bottles with contaminated soils according to the mass ratios of 1%, 2%, and 3%, respectively. These ratios were set for easy comparison considering the mass ratio of SNZVI to biochar (i.e., 1:2) in the biochar-based SNZVI. After mixing the soil and materials thoroughly, 60 mL of deionized (DI) water (120%) was used to maintain the flooded anaerobic condition. For the experimental control group, the same amount of DI water was added into soils. Triplicates were run for all treatments, and then cultured for 60 days at room temperature. The polyethylene bottles were weighed and DI water was added daily to the bottles to maintain a constant weight. After 60 days, the soil samples were retrieved, freeze-dried, ground, and passed through a 100-mesh nylon sieve prior to analysis. Before drying process, soil sub-samples were collected and stored at −80 °C for the analysis of microbial community.

### 2.3 Soil analysis and characterization of immobilization efficiency

The analytical methods of soil parameters, including soil pH, electrical conductivity (EC), dissolved organic carbon (DOC), soil organic matter (SOM), $CaCl_2$-extractable Cd concentration, available phosphorus (AP), available potassium (AK), nitrate, ammonium, sequential extraction procedure for Cd fractionation, and HCl-extractable Fe(II) concentration, are presented in Text S1 of the Supplementary Materials. The characterization methods of immobilization performance of Cd in soils are displayed in the Supplementary Materials (Text S2). Since the soil is a complex system, the relatively simple batch adsorption experiment was used to study the interaction between Cd and SNZVI/BC. Furthermore, to clarify the immobilization mechanisms of Cd by SNZVI/BC, the crystal structures of SNZVI/BC and reacted products were determined using X-ray diffraction (XRD) (Rigaku Ultima IV, Japan) in the range of 10–70° (2 theta). Moreover, the probable forms of various elements in the surface of materials after reaction were characterized by X-ray photoelectron spectrometer (XPS) (K-Alpha+, Thermo Scientific, USA).

### 2.4 Bacterial community and diversity analysis

For DNA extraction from soil samples and high-throughput sequencing of bacterial 16S rRNA genes, the detailed information is given in the Supplementary Materials (Text S3).

### 2.5 Statistical analysis

Excel 2016 was used to sort the experimental data. Analysis of variance (ANOVA) and Duncan's multiple comparison test were used to analyze the significance of differences between various treatments based on IBM SPSS statistic (version 27). The significance level (α value) was set as 0.05. The relevant data statistics of the microbial community in the soil was completed using the cloud platform provided by Majorbio (Shanghai, China). Origin 2021 and Coreldraw 21.0 were used for graphic plotting.

## 3 Results and discussion

### 3.1 Bioavailability and fractionation of Cd in the contaminated soil

The results of material characterization have been displayed in our previous study (Zhang et al. 2023c). The bioavailability, species distribution, and transformation of Cd in contaminated paddy soils after addition of BC, SNZVI, and SNZVI/BC are shown in Fig. 1. As can be seen, applications of individual SNZVI and biochar non-significantly altered the concentrations of available Cd in the treated soils. However, the addition of the composite biochar-based SNZVI significantly lowered the concentration of available Cd in contaminated soils from 14.9 (control group) to 9.9 mg $kg^{-1}$ ($P < 0.05$) with an immobilization efficiency of 33.3%, which indicated that a synergistic effect occurred. Further, the sequential extraction result indicated that the proportion of the exchangeable part of Cd in soils decreased from 50.3% to 48.4–46.5% with the addition of SNZVI, BC, and SNZVI/BC. The composite SNZVI/BC preformed best in terms of reducing the exchangeable Cd concentrations in soils. Uniformly, the carbonate-bound and residual Cd concentrations in the soils treated by SNZVI/BC also increased the greatest in the treatments. To be specific, the proportions of the carbonate-bound and residual Cd in soils increased from 20.1 to 20.9% and from 8.1 to 10.3%, respectively, when compared with

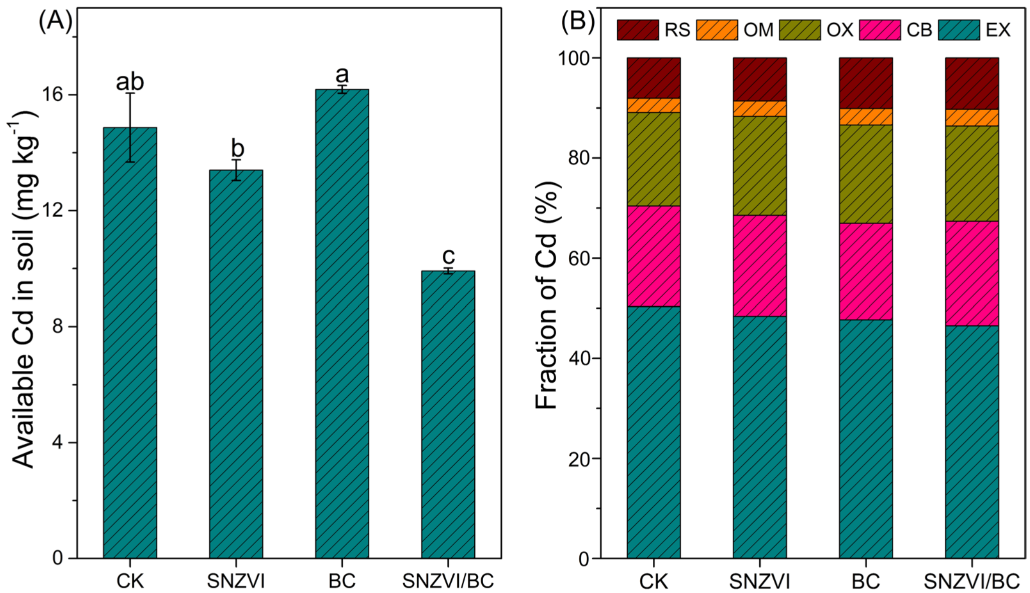


**Fig. 1** Changes in concentrations of available cadmium (Cd) in contaminated paddy soils (**A**) and its speciation distribution (**B**) after remediation by biochar (BC), sulfidized nano-sized zero valent iron (SNZVI), and biochar-based SNZVI (SNZVI/BC). Different lowercases indicate significant differences between different treatments ($P < 0.05$). *EX* exchangeable specie, *CB* carbonate-bound specie, *OX* Fe–Mn oxide-bound specie, *OM* organic material-bound specie, *RS* residual specie

the control group. These results indicated that use of SNZVI/BC can facilitate the transformation of the labile Cd fraction to the more stable fraction in contaminated soils, in favor of remediation of Cd-contaminated paddy soils. Similarly, the percentage of exchangeable fraction in total Cd also decreased by 24.2%, yet percentages of other fractions in total Cd enhanced after sulfur-iron co-modified biochar was applied into the non-rhizosphere soil (Rajendran et al. 2019). Moreover, amendment of sulfur-iron functionalized biochar weakened the available Cd (i.e., diethylenetriaminepentaaceticacid-extractable Cd) concentrations in soils by 70.3% for the simulated Cd-contaminated soil (Qu et al. 2022). Overall, the biochar-based SNZVI can effectively immobilize Cd in contaminated soils and performed better than the individual BC and SNZVI, showing a synergistic effect.

### 3.2 Change in soil physicochemical properties

The addition of immobilization materials also resulted in the change in the soil physicochemical properties, which had an indirect influence on the bioavailable Cd concentration in soils (Zhang et al. 2023a). Therefore, the changes in soil physicochemical properties after remediation were studied, and the results are shown in Fig. 2. It can be seen that soil pH significantly increased from 6.33 ± 0.02 (the control group) to 6.86 ± 0.04 for the SNZVI-treated soil, to 6.46 ± 0.01 for the BC-treated soil, and to 7.47 ± 0.02 for the SNZVI/BC treatment (Fig. 2A). The increasing effect of biochar can be mainly due to its own alkaline substance. For the SNZVI and SNZVI/BC treatments, the increase in soil pH could be ascribed to the interaction of NZVI with $O_2$ and $H_2O$, producing $OH^-$ via Eq. (1) and thus increased soil pH (Liu et al. 2022).

$$2Fe^0 + O_2 + 2H_2O \rightarrow 2Fe^{2+} + 4OH^-. \tag{1}$$

As can be seen from Fig. 2B, the addition of SNZVI and SNZVI/BC significantly improved EC values from 13.37 ± 0.56 μS $cm^{-1}$ to 29.07 ± 1.76 μS $cm^{-1}$ and to 95.87 ± 2.64 μS $cm^{-1}$, respectively, indicating that their supplementation significantly increased contents of soluble nutrients in soils and provided beneficial nutrient conditions to crops (Wang et al. 2021b, c). BC treatment, on the other hand, reduced EC value in soils, which can be attributed to the lower EC values in pinewood-derived biochars (Zhang et al. 2023a). For the change in contents of SOM, the addition of BC and SNZVI/BC significantly increased the concentrations of SOM from 3.08 to 3.41% and to 3.43%, respectively, which was because biochar is a carbonaceous material (Fig. 2C). Moreover, the concentrations of CEC of stabilization materials can reflect its absorption ability to cationic pollutants e.g. Cd(II), and the higher CEC is conducive to stabilization of potentially toxic elements in soils (Song et al. 2017). The addition of SNZVI and biochar-based SNZVI significantly increased contents of CEC in soils from 30.64 ± 0.19 cmol $kg^{-1}$ to 33.87 ± 0.17 cmol $kg^{-1}$ and to 41.29 ± 0.65 cmol $kg^{-1}$,

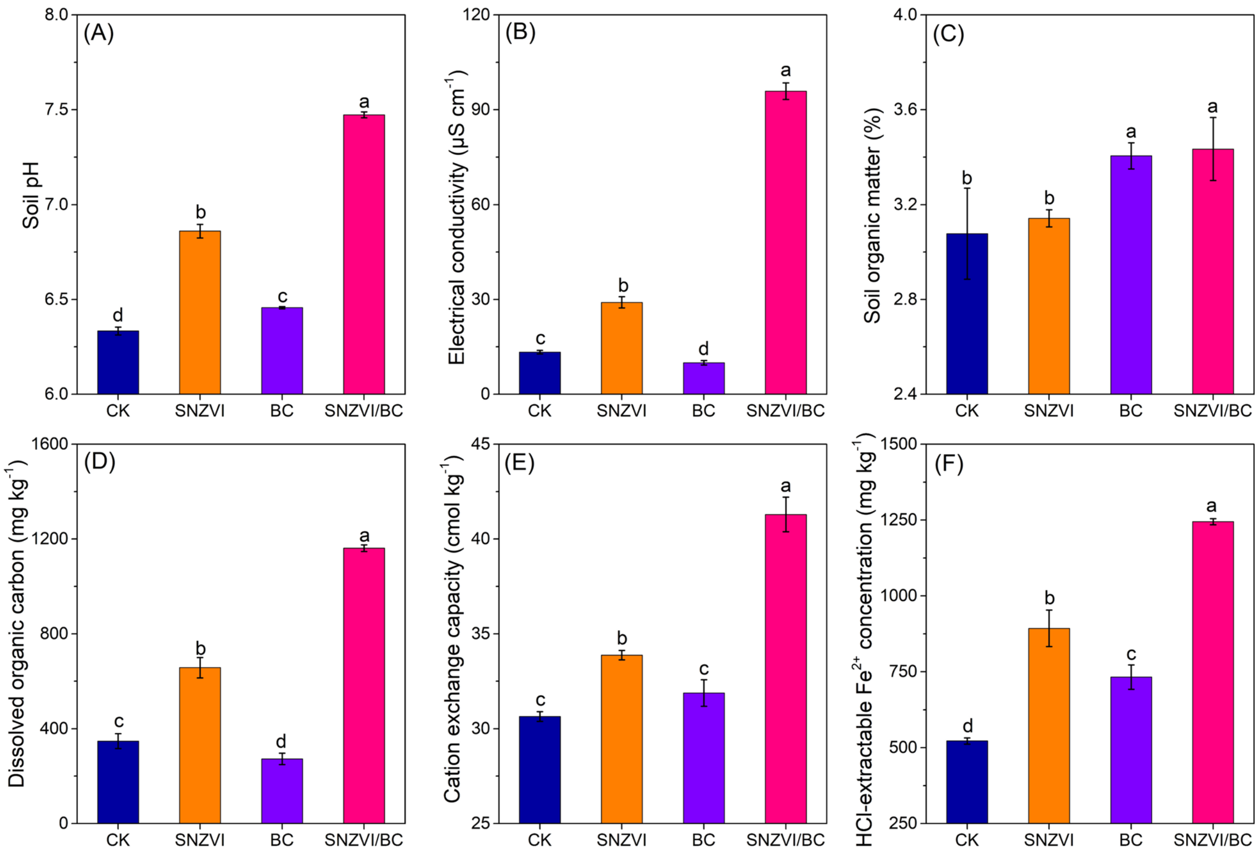

**Fig. 2** The changes in physicochemical properties in soils after remediation by sulfidized nano-sized zero-valent iron (SNZVI), biochar (BC), and biochar-supported sulfidized nano-sized zero-valent iron (SNZVI/BC). Soil pH (**A**), electrical conductivity (**B**), soil organic matter (**C**), dissolved organic matter (**D**), cation exchange capacity (**E**), and HCl-extractable $Fe^{2+}$ concentration (**F**). Different lowercases indicate significant differences between different treatments ($P < 0.05$)

respectively (Fig. 2E), which may be caused by the release of ferrous and ferric Fe from the surface of SNZVI (Liu et al. 2021) and production of ammonium.

In addition, the supplementation of SNZVI and biochar-based SNZVI significantly increased the concentrations of DOC in soils ($P < 0.05$) from $347.7 \pm 31.4$ mg $kg^{-1}$ (control group) to $657.1 \pm 42.5$ mg $kg^{-1}$ and $1161.0 \pm 14.0$ mg $kg^{-1}$, respectively (Fig. 2D). This may be due to an increase in soil pH induced by SNZVI and biochar-based SNZVI, which promoted the desorption of DOC molecules from the surface of soil particles (Hanke et al. 2013). The increase in DOC can provide available carbon resource to soil microorganisms and promote their growth, improving nutrient cycling in contaminated soils. On the contrary, the supplementation of BC significantly decreased the DOC concentrations from $347.27 \pm 31.42$ to $272.73 \pm 24.28$ mg $kg^{-1}$, which can be because of the adsorption of BC considering its high preparation temperature (700 °C). It was reported that high-temperature biochars had greater sorption capacities for DOC than biochars prepared at lower temperatures (Eykelbosh et al. 2015). It is also possible that the application of biochar into soils stimulated the growth of microorganisms, promoting the decomposition and mineralization of DOC by microorganisms, thus reducing the DOC contents in soils.

As can be seen in Fig. 2F, the concentrations of available Fe(II) in soils were significantly greater than those in the control group after addition of three materials ($P < 0.05$). Similarly, addition of biochar enhanced the available Fe(II) contents in paddy soils (Li et al. 2023). Moreover, the higher available Fe(II) contents for supplementation of SNZVI and biochar-based SNZVI can be because of the stimulation of iron-reducing bacteria in soils by SNZVI and biochar-based SNZVI, facilitating the reduction of Fe(III) minerals by microorganisms in soils (Liu et al. 2022). The greatest content of available Fe(II) for SNZVI/BC treatment can be resulted from the graphitic carbon matrix of biochar, as an electron shuttle, promoting the extracellular electron transfer of iron-reducing bacteria to Fe(III) oxide minerals including oxidative products of zero-valent iron and the endogenous Fe(III) oxides minerals in soils (Liu et al. 2022; Zhang et al. 2022b, 2023a). It was reported that poorly crystalline secondary Fe(II)-containing minerals played an important role in immobilizing Cd in soils (Muehe et al. 2013; Liu et al. 2022).

### 3.3 Change in available nutrients in soils

The effects of SNZVI, BC, and biochar-based SNZVI on the concentrations of available nutrients in soils are shown in Fig. 3. The addition of SNZVI, BC, and biochar-based SNZVI significantly increased the concentration of $NH_4^+$ in soils ($P<0.05$). To be specific, the content of $NH_4^+$ in contaminated soils increased by 64.9%, 20.0%, and 114.2%, respectively, in comparison to the control group (Fig. 3A). The reason could be the coupling of microbial reduction of Fe(III) minerals and nitrogen fixation mediated by microorganisms (e.g., *Clostridiales*) (Masuda et al. 2021). Moreover, microbial mineralization of dissolved organic nitrogen may also contribute to the production of $NH_4^+$ in soils (Liu et al. 2023b). In addition, the dissimilatory nitrate reduction to ammonium (DNRA) process affected by *Bacillus* could also contribute to the production of $NH_4^+$ because the coupled application of biochar and ZVI can synergistically facilitate the DNRA process (Yuan et al. 2022; Chen et al. 2023b). On the other hand, the contents of nitrate in soils were significantly improved after supplementation of SNZVI and biochar-based SNZVI ($P<0.05$) in comparison to control group (Fig. 3B). Specifically, the increase amplitude of $NO_3^-$ contents in soils were 65.7% and 140.2%, respectively. Generally, NZVI added into soils can be completely oxidized to iron oxides, e.g., crystalline maghemite (γ-$Fe_2O_3$) and magnetite ($Fe_3O_4$) (Wang et al. 2021a). In this regard, ferrihydrite, lepidocrocite, goethite, and magnetite as the oxidative products of NZVI were identified in the same proportions, which had no concern with the amount of the oxidized NZVI (Liu et al. 2023a, b; Mitzia et al. 2023). The improved contents of nitrate can be resulted from the coupled reaction of microbial reduction of Fe(III) minerals with the anaerobic oxidation of ammonium (Xu et al. 2020) and the traditional nitrification process of $NH_4^+$ in soils (Ma et al. 2021). Moreover, biochar-based SNZVI performed better, probably attributed to the mediation role of biochar as an electron shuttle in the redox transformation of Fe and N in soils (Hu et al. 2021).

Moreover, supplementation of SNZVI significantly decreased the content of available P in soils from $5.81 \pm 0.22$ to $4.05 \pm 0.38$ mg kg$^{-1}$, which can be explained by the formation of iron phosphate minerals (Zhang

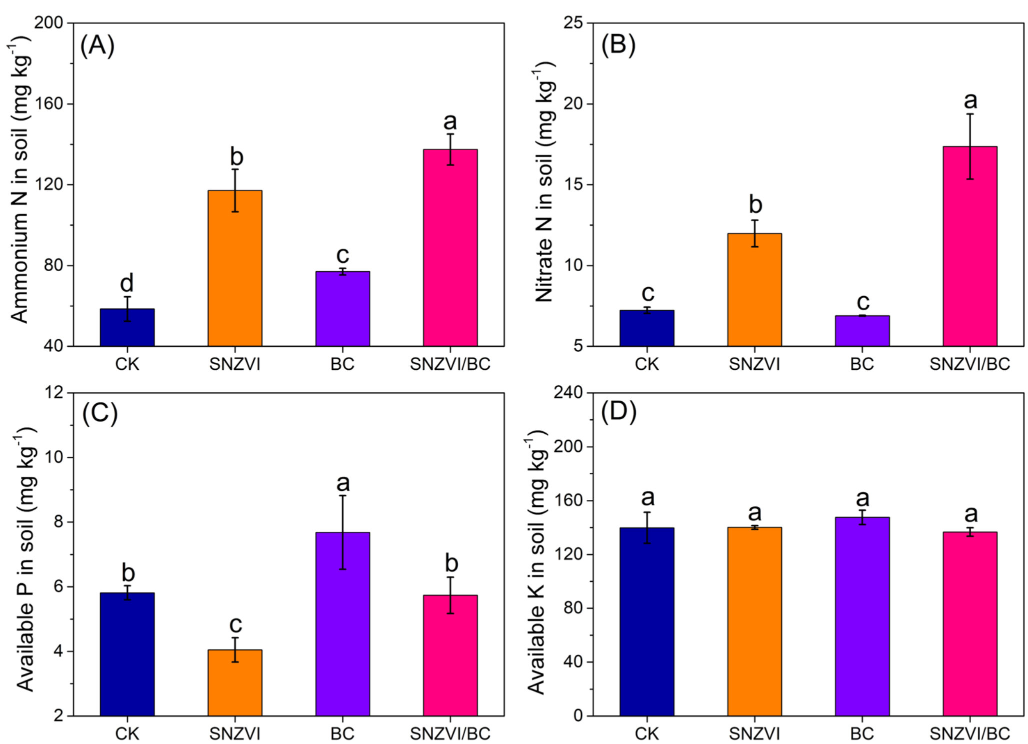


**Fig. 3** The changes in available nutrients [ammonium (**A**), nitrate (**B**), available phosphorus (**C**), and available potassium (**D**)] in soil after application of sulfidized nano-sized zero-valent iron (SNZVI), biochar (BC), and biochar-based sulfidized nano-sized zero-valent iron (SNZVI/BC). Different lowercases indicate significant differences between different treatments ($P<0.05$)

et al. 2022c). On the contrary, input of biochar significantly increased available P concentrations in soils from $5.81 \pm 0.22$ to $7.68 \pm 1.14$ mg $kg^{-1}$ under the anaerobic condition (Fig. 3C). This can be because biochar application resulted in significant improvement of the relative abundance of phosphorus-solubilizing bacteria (Sui et al. 2022). Furthermore, the formation of iron phosphate minerals compromised the enhancement effect of biochar towards available P in soils, which led to the non-significant change for the available P content in the SNZVI/BC treatment. On the other hand, the addition of three immobilization materials unaffected significantly available K contents in contaminated soils, which is inconsistent with the previous study (Zhang et al. 2023c). This could be related to the inherent difference of soil type. Overall, the biochar-based SNZVI performed better in terms of the improvement of available nutrients, especially ammonium and nitrate in soils than individual SNZVI and BC, which was conducive to crop growth.

### 3.4 Response on microbial community after remediation

In Sects. 3.2 and 3.3, we assumed that the changes in available nutrients and physicochemical properties in soils can be related to the response on microbial community. Therefore, the microbial community and diversity in all soils were investigated to elucidate the role of microorganism in changes in available nutrients, physicochemical properties, and immobilization of Cd in soils after the application of SNZVI, BC, and SNZVI/BC. The alpha richness and diversity indices of bacterial 16S rRNA gene in soils are showed in Fig. S1. The addition of SNZVI and BC non-significantly affected on the richness and diversity of bacteria in soils. However, the supplementation of biochar-based SNZVI significantly reduced the Ace, Chao, and Simpson indices ($P < 0.05$), indicating the decrease in the richness and diversity of bacterial community in soils (Lyu et al. 2022). The decrease in abundance and diversity may be due to the toxicity of iron ion released from NZVI to bacteria in soils (Cai et al. 2019). Moreover, the biochar-based SNZVI-induced decrease in the richness and diversity of bacterial community in soils can be because the SNZVI/BC significantly stimulated specific bacteria in the soils and improved their relative abundances via competition with other bacteria (Xue et al. 2022). Furthermore, some reported works demonstrated that soil bacteria can participate in Cd immobilization in soils, and stabilization materials can indirectly affect bioavailability of Cd via impacting the bacterial community (Liu et al. 2021; Xu et al. 2022; Xue et al. 2022). Therefore, we further analyzed the composition of soil bacterial community at phylum and genus levels to identify the role of soil bacteria in the change in soil physicochemical properties, nutrient biogeochemical cycling, and Cd immobilization.

On the phylum level (Fig. 4A), the dominant bacterial phyla in the control group were *Actinobacteriota*, *Bacteroidota*, and *Firmicutes*, and their relative abundances were 17.79%, 25.33%, and 29.04%, respectively, which agrees with the previous study (Liu et al. 2020). The supplementation of SNZVI and SNZVI/BC increased the relative abundances of *Firmicutes* and *Halanaerobiaeota*. To be specific, the relative abundance of *Firmicutes* enhanced from 29.04 to 42.53% for the SNZVI treatment and to 63.53% for the SNZVI/BC treatment. The relative abundance of *Halanaerobiaeota* improved from 0.01 to 2.24% and 4.34% for SNZVI and SNZVI/BC treatments, respectively. Phylum *Firmicutes* carries a variety of potentially toxic elements resistance genes, which is conducive to their rapid reproduction in potentially toxic element-polluted environments (Liu et al. 2021). In addition, *Firmicutes* is also the dominant taxonomic phylum of Fe(III)-reducing bacteria in anoxic soils (Zhang et al. 2023b). *Halanaerobiaeota* could enhance the nitrogenous substance metabolic pathway and decrease $NH_3$ emission (Xu et al. 2023c). SNZVI and SNZVI/BC treatments reduced the abundance of *Proteobacteria* compared to the control group from 6.04 to 3.54% and 2.72%, respectively. Phylum *Proteobacteria* is one of the dominant bacteria in contaminated sediments and has been shown to be involved in the immobilization of potentially toxic elements (Liu et al. 2020). SNZVI/BC treatment resulted in a 76.07% decrease compared to the control group with the relative abundance of 25.33% for phylum *Bacteroidota*. Supplementation of biochar-based SNZVI lowered the abundance of *Bacteroidota* and *Proteobacteria* can be because of the competition for nutrients from the fast-growing *Firmicutes*.

At the genus level (Fig. 4B), the supplementation of biochar-based SNZVI significantly reduced the relative abundance of *norank_f__Bacteroidetes_vadinHA17*, which is consistent with the variation of the abundance of phylum *Bacteroidota*. In comparison to the control group, the addition of SNZVI and biochar-based SNZVI significantly increased the relative abundance of *Lentimicrobium*, *Clostridium_sensu_stricto_10*, *Ruminiclostridium*, *Lutispora*, *Oxobacter*, *norank_f__Halobacteroidaceae*, *Sedimentibacter*, *Desulfitobacterium*, *Bacillus*, and *Desulfosporosinus*. Genus *Lentimicrobium* was reported as key species metabolizing both nitrogen and DOM in sediments (Wang et al. 2022), hydrolytic acid-producing bacteria (Xu et al. 2023b), and denitrifying bacteria (Wang et al. 2023c). *Ruminiclostridium* was an anaerobe found in decayed plants and could decompose hemicellulose, thus increasing the DOC concentration (Aksorn et al. 2022). *Lutispora*,

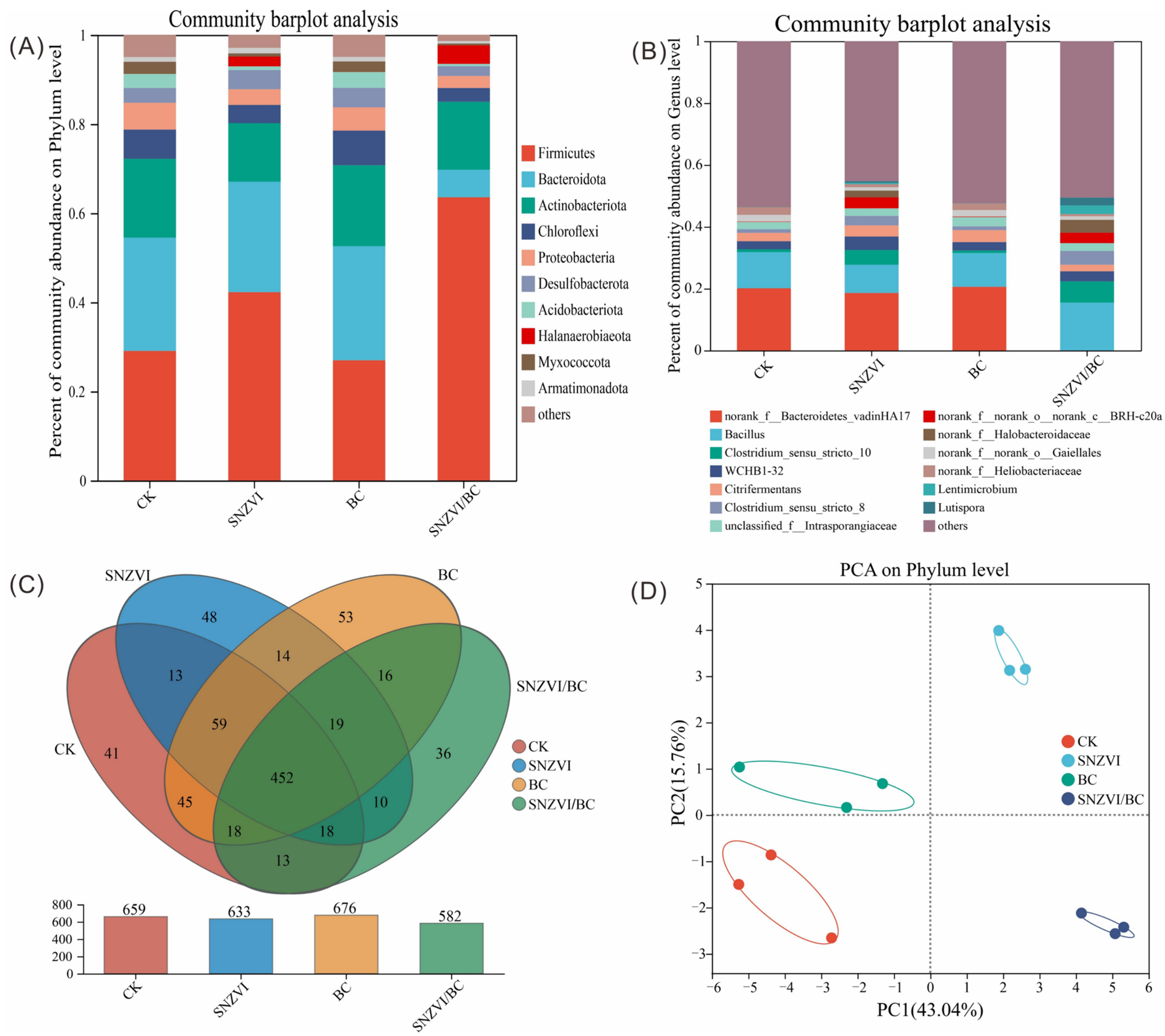


**Fig. 4** The response of microbial community structure after application of sulfidized nano-sized zero-valent iron (SNZVI), biochar (BC), and biochar-based sulfidized nano-sized zero-valent iron (SNZVI/BC). **(A)** Phylum level; **(B)** genus level; **(C)** Venn diagram; **(D)** principal component analysis (PCA) on phylum level

a protein-degrading anaerobes, can decompose protein to yield volatile fatty acid (e.g., acetate, isobutyrate, and propionate), ammonium, and hydrogen sulfide (Chen et al. 2018). The increase in abundance of genera *Oxobacter* can explain the enhancement of butyrate, propionate, and caproate concentrations in anaerobic digestion (Zhang et al. 2022a). *Halobacteroidaceae* bacteria were previously discovered in saline sediments or soils, and confirmed as moderate halophilic bacteria that can ferment glucose into volatile fatty acid (Ali et al. 2022). The bacterial genera *Clostridium_sensu_stricto_10* and *Sedimentibacter* were reported to be responsible for most long-chain fatty acids degradation to biomethane precursors (Usman et al. 2022). Moreover, supplementation of biochar-based SNZVI increased the relative abundance of *Bacillus*. *Bacillus* has also been reported to own multiple functions, such as potentially toxic element-resisting and immobilizing traits, dissimilated Fe(III) reduction, dissimilatory nitrate reduction to ammonium, and nitrogen fixation (Han et al. 2022). In addition, addition of biochar significantly increased the relative abundance of *Citrifermentans* and *Fonticella* by 44.3% and 31.8% with the comparison to control group. *Citrifermentans* and *Fonticella* could contribute to phosphate dissolution as phosphate-solubilizing bacteria, which is consistent with the increase available P in soils (Qi et al. 2023; Teng et al. 2023).

Venn diagrams can be used to display the number of common or unique species in different treatments. The results indicated that the addition of SNZVI and biochar-based SNZVI lowered the total species of soil microorganisms (Fig. 4C), with the number of specific bacterial genera in SNZVI/BC and CK treatments being 36 and 41, respectively, and the number of unique species in SNZVI/BC treatment being lower than that in the control group, which may be due to the enrichment of some functional microorganisms in soils owing to the supplementation of biochar-based SNZVI. In addition, the results of PCA indicated that the first two principal components accounted for 58.8% of the total variation. Further, the distance of inter-treatments was significantly higher than the distance of intra-treatments according the scatter plot of samples' scores (Fig. 4D), showing that the supplementation of SNZVI, BC, and biochar-based SNZVI had significant effects on soil microbial community structure and composition.

### 3.5 Relationship between environmental factors and microbial communities

Changes in soil physicochemical properties induced by remediation materials may have an important impact on the microbial community composition in soils. As feedback, the changed microbial community can play an important role in influencing physicochemical properties in soils, such as immobilization of potentially toxic elements, nutrient availing and cycling, and changes in physicochemical properties in soils. RDA and Pearson correlation analysis were used to investigate the relationships among physicochemical properties, bioavailable Cd, and microbial communities in soils (Fig. S2). The results indicated that the microbial community in soils was significantly impacted by soil pH ($R^2=0.96$, $P=0.001$), CEC ($R^2=0.95$, $P=0.001$), EC ($R^2=0.97$, $P=0.002$), DOC ($R^2=0.98$, $P=0.001$), nitrate ($R^2=0.97$, $P=0.001$), ammonium ($R^2=0.84$, $P=0.002$), and available Cd ($R^2=0.91$, $P=0.001$). Therefore, the above-mentioned soil parameters (i.e. soil pH, CEC, EC, DOC, nitrate, ammonium, and available Cd) had important effects on the microbial community in soils.

The results of Pearson correlation analysis between soil parameters and the relative abundance of microorganism on phylum or genus levels are showed in Fig. 5. At the phylum level (Fig. 5A), the abundances of *Firmicutes* and *Halanaerobiaeota* were significantly positively correlated with ammonium, EC, CEC, available Fe(II), DOC, pH, and nitrate in soils, respectively ($P<0.05$). On the contrary, the significant negative correlation between available Cd concentration and the abundances of *Firmicutes* or *Halanaerobiaeota* were observed ($P<0.05$). At the genus level (Fig. 5B), the significant positive correlations between available Fe(II) concentration and respective abundances of *Clostridium_sensu_stricto_8*, *Clostridium_sensu_stricto_9*, and *Bacillus* in soils were

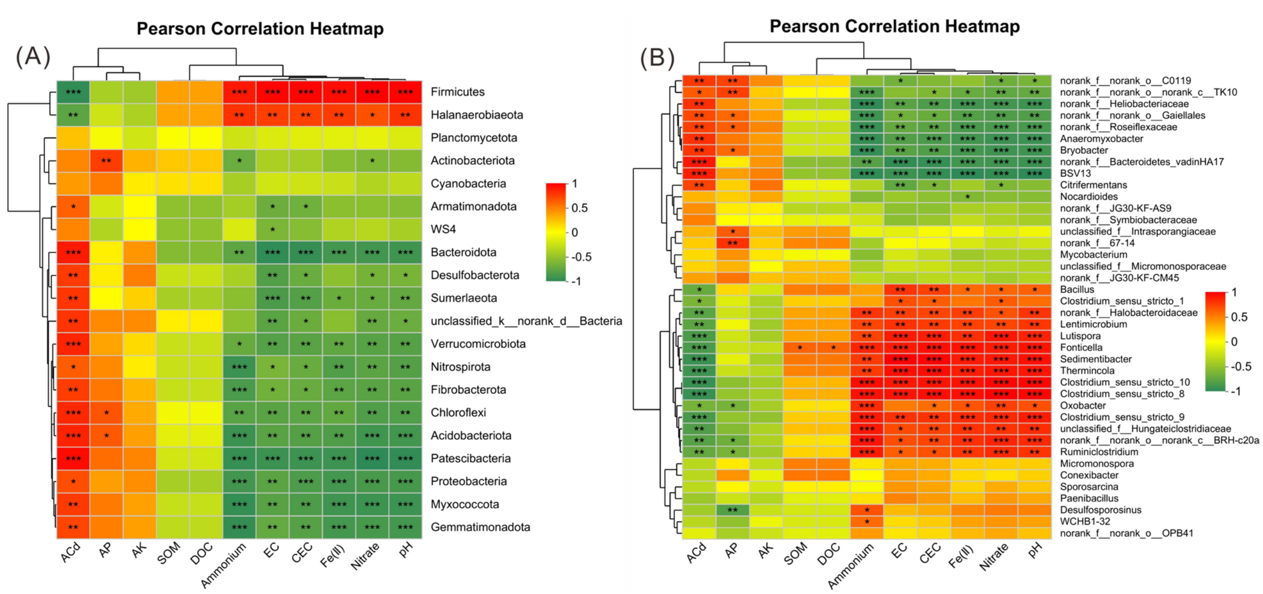


**Fig. 5** Pearson correlation analysis between physicochemical properties of soils and the relative abundance of bacteria at phylum level (**A**) and genus level (**B**). *Fe(II)* concentration of HCl-extractable ferrous Fe, *EC* electrical conductivity, *CEC* cation exchange capacity, *DOC* dissolved organic carbon, *AP* available phosphorus, *AK* available potassium, *SOM* soil organic matter, *ACd* the concentration of available Cd in soils. $P<0.05$ (*); $P<0.01$ (**); $P<0.001$ (***)

observed ($P<0.05$), which could imply that these genera participated in the reduction of Fe(III) minerals by microorganisms (Xue et al. 2022). The abundances of *Lutispora*, *norank_f__Halobacteroidaceae*, and *Lentimicrobium* were significantly positively correlated with ammonium and nitrate concentrations in soils, respectively, indicating that they can be involved in nitrogen transformation (e.g., denitrification, nitrogen fixation, and degradation of dissolved organic nitrogen) (Chen et al. 2018; Chi et al. 2021; Zhao et al. 2022). The significant positive correlation between the DOC concentration in soils and the abundance of *Ruminiclostridium* was observed ($P<0.05$). *Ruminiclostridium* was reported as an anaerobic, cellulose- and hemicellulose-decomposing bacterium capable of degrading and catabolizing several different polysaccharides (Kampik et al. 2020). This suggested that an improvement in the abundance of *Ruminiclostridium* can increase the DOC content in soils, which also supported the result of Sect. 3.2. On the contrary, the available Cd concentration was significant negative correlated to the abundances of *Lutispora*, *norank_f__Halobacteroidaceae*, *Lentimicrobium*, *Ruminiclostridium*, *Clostridium_sensu_stricto_9*, *Bacillus*, *Oxobacter*, and *Sedimentibacter*, *Clostridium_sensu_stricto_8*, respectively ($P<0.05$). This observation is consistent with the results of phylum, possibly implying that the supplementation of biochar-based SNZVI reduced the bioavailability of Cd and thus lowered its toxicity to microbes in soils, which promoted the growth and proliferation of these bacteria in soils (Xue et al. 2022; Zhang et al. 2023a). Overall, the enriched beneficial microorganisms made an important contribution to the transformation of nitrogen, carbon metabolism, Cd immobilization, reduction of ferric iron minerals, and the change in physicochemical properties in soils. Further, the supplementation of biochar-based SNZVI significantly changed the soil physicochemical properties, and then changed the bacterial community composition in soils, which enabled the enrichment of *Bacillus* with Cd immobilization ability, and thus promoted stabilization of Cd in contaminated soils.

### 3.6 Functional prediction of bacterial communities

Results of functional prediction of bacterial communities in soils can further validate their role in element biogeochemical cycling and toxic metal stabilization. The heat map of bacterial community function predicted according to FAPROTAX database is shown in Fig. 6. The results indicated that the functional abundances of iron respiration, sulfur respiration, thiosulfate respiration, sulfite respiration, sulfate respiration, sulfur-containing compound respiration, and fermentation were higher in the SNZVI- and biochar-based SNZVI-treated soils than those in the control and BC-treated soils. Moreover, biochar-based SNZVI treatment significantly improved the abundances of some functions e.g., nitrogen respiration, nitrate respiration, nitrite respiration, nitrate denitrification, nitrite denitrification, and nitrous oxide denitrification. In this regard, a previous study indicated that the addition of SNZVI/BC could provide a large number of electron donors for the denitrification reaction, which promoted the complete denitrification and reduced the fluxes of $N_2O$ (Kong et al. 2023a, b). Moreover, NZVI can inhibit the $N_2O$ production during denitrification and promoted the $N_2O$ biological consumption via regulating the activities of soil nitrate reductase (Nar), nitrite reductase (Nir), nitric oxide reductase (Nor), and nitrous oxide reductase (Nos) under the control of functional genes (*narG*, *nirS*/*nirK*, *norB*, and *nosZ*) (Su et al. 2023). Furthermore, the addition of biochar resulted in a higher ratio of *nosZ*/(*amoA* + *nirS* + *nirK*), leading to decreased $N_2O$ emission (Liao et al. 2021), In addition, ferrous sulfide can supply electrons for $NO_x^-$–N and $N_2O$ reductions by stimulating more abundant sulfur-oxidizing denitrifiers (e.g., *Thiobacillus*) (Wang et al. 2023a, b, c, d). This further supported the results of available nutrients and physicochemical properties in the SNZVI and biochar-based SNZVI treatments.

### 3.7 Mechanism of Cd immobilization

#### 3.7.1 Adsorption of SNZVI/BC

Biochar-based SNZVI can synergistically immobilize Cd in contaminated paddy soils. Therefore, the involved immobilization mechanism was further clarified. The XPS spectra of C, O, Fe, S, and Cd before and after immobilization of Cd by SNZVI/BC are shown in Fig. 7. The fine spectrum of C 1 s before immobilization could be disassembled into C=C/C–C (283.92 eV), C–O–H/C–O (284.85 eV), C=O (286.30 eV), and –COOR (288.28 eV) (Yin et al. 2023) (Fig. 7B). After immobilization, the positions and areas of these characteristic peaks experienced slight variation. Similarly, the spectrum of O 1 s was deconvoluted into $O^{2-}$ (FeOOH) (530.20 eV), C–O (531.40 eV), and C=O (532.42 eV) before immobilization (Zhou et al. 2018) (Fig. 7C). The slight alteration of these characteristic peaks was observed after immobilization. These results indicated that the functional groups with oxygen on the surface of biochar-based SNZVI participated in Cd immobilization via surface complexation.

Further, five deconvoluted characteristic peaks were observed for the spectrum of Fe 2p at 707.00, 710.30, 711.98, 723.53, and 724.96 eV, matching NZVI, ferrous iron of Fe $2p_{3/2}$, ferric iron of Fe $2p_{3/2}$, ferrous iron of Fe $2p_{1/2}$, and ferric iron of Fe $2p_{1/2}$ before adsorption (Tian et al. 2023). After adsorption, the positions and areas of these characteristic peaks underwent slight

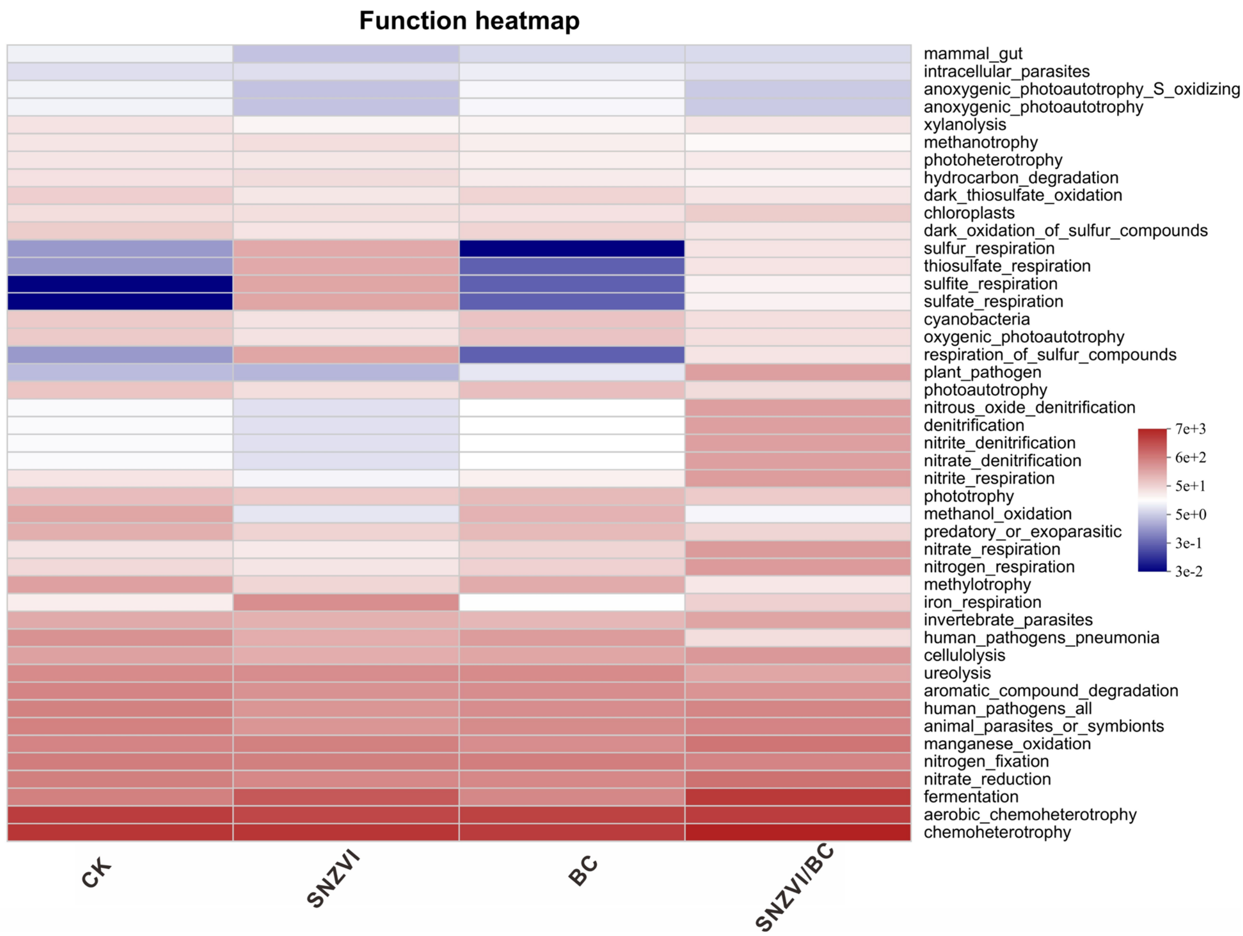


**Fig. 6** The function heatmap of microbial community predicted according to FAPROTAX database after application of sulfidized nano-sized zero-valent iron (SNZVI), biochar (BC), and biochar-based sulfidized nano-sized zero-valent iron (SNZVI/BC)

shift, indicating that functional groups with Fe participated in Cd stabilization (Zhang et al. 2023c). Before immobilization, the spectrum of S 2p was divided into $S^{2-}$ (161.01 eV), $S_2^{2-}$ (163.03 eV), $S_n^{2-}$ (164.21 eV), and $SO_4^{2-}$ (168.10 eV). After immobilization, three sub-peaks were observed at 161.30, 162.95, and 168.14 eV, respectively, which were confirmed as CdS, $FeS_x$, and $SO_4^{2-}$, respectively (Yin et al. 2023). This indicated that the displacement reaction between Cd(II) ion and iron sulfide and the formation of CdS precipitate effectively facilitated Cd immobilization. For the spectrum of Cd 3d, two sub-peaks were observed at 404.96 and 411.71 eV, respectively, which were identified as Cd-iron oxides/CdS/$CdCO_3$ and Cd–O binding (Yin et al. 2023; Zheng et al. 2023). This indicated that adsorption of iron oxides and precipitation participated in Cd immobilization. Further, the XRD spectrum of SNZVI/BC after adsorption of Cd indicated that the formation of CdS and $CdCO_3$ precipitates was involved in Cd immobilization (Fig. S4), which was in agreement with the result of XPS analysis.

#### *3.7.2 Effect of soil physicochemical properties*

Addition of functional materials induced changes in soil physicochemical properties, which can indirectly influence bioavailable Cd concentrations in soils (Ma et al. 2023). The results of Pearson correlation analysis indicated that EC, soil pH, DOC, Fe(II), CEC, nitrate, and ammonium were inversely proportional to available Cd in soils, respectively (Fig. S3). Increase in soil pH can facilitate the deprotonation of oxygen-containing functional groups of surface of soil particles, enhancing the electrostatic attraction between $Cd^{2+}$ and soil particles (Ma et al. 2023). Moreover, the increase in soil pH from 6.33 to 7.47 was also in favor of the generation of Cd carbonate precipitates ($CdCO_3$), lowering the available Cd in soils (Lu et al. 2022), which was consistent with the result of the fraction's transformation. In this regard, although the carbonate bound Cd is sensitive to pH changes, there was only a 0.8% increase in carbon bound Cd (Fig. 1) when the pH ranged from 6.33 to 7.47. The reason can be that the solubility constant

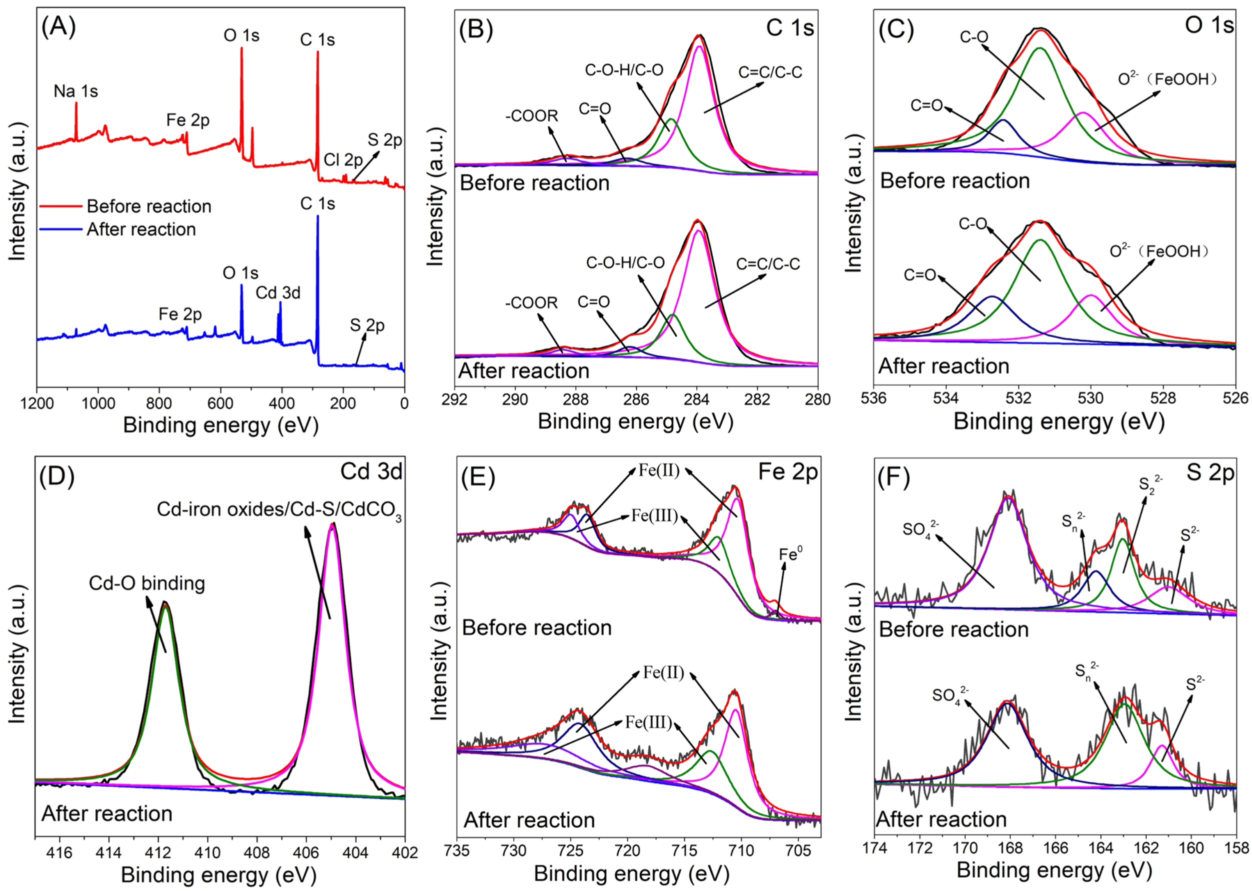


**Fig. 7** The XPS spectra of total survey scans (**A**). The high-resolution XPS spectra of C 1 s (**B**), O 1 s (**C**), Cd 3d (**D**) Fe 2p (**E**), and S 2p (**F**) of biochar-based sulfidized nano-sized zero-valent iron (SNZVI/BC) before and after cadmium (Cd) stabilization

($K_{sp}$) of Cd sulfide ($7.9\times10^{-27}$) is lower than that of $CdCO_3$ ($5.2\times10^{-12}$), which facilitates the transformation of $CdCO_3$ to CdS considering the abundant sulfur in the soil under the current anaerobic condition. The inverse correlation between Fe(II) concentration and available Cd concentration and Cd immobilization could imply that secondary iron minerals formed from microbial reduction of ferric iron minerals participated in the immobilization of Cd in soils (Muehe et al. 2013; Zhang et al. 2023b). The negative correlation between available Cd and nitrate/ammonium could indicate that SNZVI/BC addition reduced bioavailability of Cd in soils, ameliorated the toxicity of Cd to soil microorganism, increased the abundance of nitrogen cycling associated bacteria, and thus facilitated the soil nitrogen cycling e.g., denitrification, nitrogen fixation, and Feammox (Chi et al. 2021; Xue et al. 2022; Chen et al. 2023b). Overall, addition of SNZVI/BC could also immobilize Cd in contaminated soils via enhancing soil pH and facilitating the formation of secondary iron minerals.

### *3.7.3 Effect of microorganism*

Microorganisms can immobilize Cd in soils, mainly through bioadsorption, bioaccumulation (Wang et al. 2023b), and microbes-induced formations of phosphate precipitates (Zhang et al. 2021a), carbonate precipitates (Wu et al. 2022), and sulfide precipitates (Wu et al. 2022). Supplementation of biochar-based NZVI increased the relative abundance of *Bacillus* by 32.6% compared with that in the control soil. A reported work showed that the two synergistic strategies (i.e., extracellular chemisorption and intracellular bioaccumulation) were involved in the removal of Cd(II) by *Bacillus* (Wang et al. 2023b). Moreover, addition of SNZVI enhanced the relative abundances of *Desulfosporosinus* and *Desulfitobacterium* by 50.7 and 4.4 times, respectively. In the soil treated by biochar-based SNZVI, the relative abundances of *Desulfosporosinus* and *Desulfitobacterium* were enhanced by 20.6 and 1.8 times when compared with the control soil. *Desulfosporosinus* and *Desulfitobacterium* were reported as sulfate-reducing bacteria (SRB) that can reduce $SO_4^{2-}$ to $S^{2-}$, which favored the formation of Cd sulfide precipitate (Wu et al. 2022, 2023b). Additionally, $SO_4^{2-}$ as one of the aged products of SNZVI and substrate of SRB can be formed after applying SNZVI into soils (Hui et al. 2022). Therefore, these stimulated functional microbes (*Bacillus*, *Desulfosporosinus*, and *Desulfitobacterium*) could also play a key role in immobilizing Cd in polluted soils.

#### *3.7.4 Effect of interaction between SNZVI and BC*

Since the synergistic effect between SNZVI and biochar was observed, and the effect of the interaction between them on Cd immobilization in soils was further discussed. Firstly, biochar as a dispersant can efficiently inhibit aggregation of SNZVI, improving the magnitude of interaction sites between SNZVI and Cd ion in soils (Gao et al. 2023). Secondly, given high fabrication temperature of biochar (700 ℃), it can be used as an electron shuttle to promote the microbial reduction of Fe(III) oxides minerals formed from corrosion of ZVI by iron-reducing bacteria, facilitating the production of secondary iron minerals (Zhang et al. 2023b). The newly-produced secondary iron minerals can effectively immobilize Cd through structural incorporation of minerals and surface adsorption (Muehe et al. 2013). Thirdly, biochar as an immobilization carrier can provide attachment sites to sulfate-reducing bacteria and iron-reducing bacteria for their survivals (Liu et al. 2023a; Si et al. 2023). This further promoted the microbial reduction of sulfate to $S^{2-}$ and the formation of Cd sulfide precipitate, thus facilitating immobilization of Cd.

## 4 Conclusion

In the present work, biochar-based SNZVI was used to remediate Cd-contaminated paddy soils. The composite biochar-based SNZVI effectively immobilized Cd in the contaminated paddy soil with an immobilization efficiency of 33.3% better than individual biochar or SNZVI, exhibiting a synergistic effect. The composite SNZVI/BC also facilitated the transformation of the labile Cd forms in the polluted soil to the more stable species. Moreover, the composite SNZVI/BC also increased soil pH, organic matter, cation exchange capacity, dissolved organic carbon, ammonium, nitrate, and available Fe(II) concentrations in the polluted soil. Furthermore, the addition of SNZVI/BC altered the bacterial community in soils, increasing the relative abundance of *Bacillus*, *Clostridium*, and *Desulfosporosinus*. The direct interaction of SNZVI/BC with Cd, the altered soil physicochemical properties, and the changed bacterial community played important roles in Cd immobilization in the contaminated paddy soil. The further pot experiment is recommended to verify the immobilization efficiency of SNZVI/BC towards Cd in the contaminated soil in future works.

## Supplementary Information

The online version contains supplementary material available at https://doi.org/10.1007/s42773-024-00349-8.

Supplementary Material 1.

**Acknowledgements**

This work was supported by Basic Research General Project of Guizhou Provincial Department of Science and Technology(ZK[2024]014), Basic Research Project of Guizhou Provincial Department of Science and Technology ([2020]1Z037), Guizhou Provincial Science and Technology Projects (Qian Ke He Support ([2022]222), Youth Talent Growth Project of Guizhou Provincial Department of Education (2024), Special Fund for Outstanding Youth Talents of Science and Technology of Guizhou Province [YQK[2023]014], and National Natural Science Foundation of China [Grant numbers 41977297; 42277040; 41977117], and Special Research Foundation of Natural Science (Special Post) of Guizhou University [(2023)04].

**Author contributions**

Yu Zhou wrote the manuscript. Lu Lv finished the experiment. Zhi Yu revised the manuscript. Bing Wang, Ruidong Yang, Miao Chen, Pan Wu, and Shengsen Wang reviewed and provided valuable comments to the manuscript. Dr. Jian Zhang have made substantial contributions to this work. All authors have reviewed the manuscript and given their permission to be named.

**Funding**

Basic Research General Project of Guizhou Provincial Department of Science and Technology(ZK[2024]014), Basic Research Project of Guizhou Provincial Department of Science and Technology ([2020]1Z037), Guizhou Provincial Science and Technology Projects (Qian Ke He Support ([2022]222), The Youth Talent Growth Project of Guizhou Provincial Department of Education (2024), Special Fund for Outstanding Youth Talents of Science and Technology of Guizhou Province [YQK[2023]014], and National Natural Science Foundation of China [Grant numbers 41977297; 42277040; 41977117], and Special Research Foundation of Natural Science (Special Post) of Guizhou University [(2023)04].

**Availability of data and materials**

Not applicable.

## Declarations

**Competing interests**

The authors declare that they have no known competing financial interests or personal relationships that could have appeared to influence the work reported in this paper.

**Author details**

[1]Key Laboratory of Kast Georesources and Environment, Ministry of Education, Guizhou University, Guiyang 550025, China. [2]Guizhou Research and Designing Institute of Environmental Sciences, Guiyang 550081, China. [3]College of Resources and Environmental Engineering, Guizhou University, Guiyang 550025, China. [4]College of Environmental Science and Engineering, Yangzhou University, Yangzhou 225127, China.

Received: 3 November 2023 Revised: 28 April 2024 Accepted: 17 May 2024
Published online: 03 June 2024

**References**

Aksorn S, Kanokkantapong V, Polprasert C, Noophan P, Khanal SK, Wongkiew S (2022) Effects of Cu and Zn contamination on chicken manure-based

bioponics: nitrogen recovery, bioaccumulation, microbial community, and health risk assessment. J Environ Manag 311:114837
Ali M, Fujii M, Ibrahim MG, Elreedy A (2022) On the potential of halophiles enriched from hypersaline sediments for biohydrogen production from saline wastewater. J Clean Prod 341:130901
Cai C, Zhao M, Yu Z, Rong H, Zhang C (2019) Utilization of nanomaterials for in-situ remediation of heavy metal(loid) contaminated sediments: a review. Sci Total Environ 662:205–217
Chen S, He J, Wang H, Dong B, Li N, Dai X (2018) Microbial responses and metabolic pathways reveal the recovery mechanism of an anaerobic digestion system subjected to progressive inhibition by ammonia. Chem Eng J 350:312–323
Chen G, Ma Y, Xu W, Chen Z, Li Z, Zhou J, Yu W (2023a) Remediation of cadmium-contaminated soil by micro-nano nitrogen-doped biochar and its mechanisms. Environ Sci Pollut Res 30:48078–48087
Chen J, Xie Y, Sun S, Zhang M, Yan P, Xu F, Tang L, He S (2023b) Efficient nitrogen removal through coupling biochar with zero-valent iron by different packing modes in bioretention system. Environ Res 223:115375
Chi Z, Ju S, Li H, Li J, Wu H, Yan B (2021) Deciphering edaphic bacterial community and function potential in a Chinese delta under exogenous nutrient input and salinity stress. CATENA 201:105212
Ding Y, Li M, Zhang Q, Zhang Y, Xia Z, Liu X, Wu N, Peng J (2023) Sulfidized state and formation: enhancement of nanoscale zero-valent iron on biochar(S-nZVI/BC) in activating peroxymonosulfate for Acid Red 73 degradation. J Environ Chem Eng 11:110114
Eykelbosh AJ, Johnson MS, Couto EG (2015) Biochar decreases dissolved organic carbon but not nitrate leaching in relation to vinasse application in a Brazilian sugarcane soil. J Environ Manag 149:9–16
Gao F, Zhang M, Ahmad S, Guo J, Shi Y, Yang X, Tang J (2023) Tetrabromobisphenol A transformation by biochar supported post-sulfidated nanoscale zero-valent iron: mechanistic insights from shell control and solvent kinetic isotope effects. J Hazard Mater 458:132028
Guo X, Xu J, He D, Bu D, Lu Y, Zhao Y, Chen Y, Tian X (2022) Combining paecilomyces variotii extracts and biochar for the remediation of alkaline Cd-contaminated soil. Biomass Convers Biorefin. https://doi.org/10.1007/s13399-022-03308-0
Han H, Wu X, Hui R, Xia X, Chen Z, Yao L, Yang J (2022) Synergistic effects of Cd-loving *Bacillus* sp. N3 and iron oxides on immobilizing Cd and reducing wheat uptake of Cd. Environ Pollut 305:119303
Hanke A, Cerli C, Muhr J, Borken W, Kalbitz K (2013) Redox control on carbon mineralization and dissolved organic matter along a chronosequence of paddy soils. Eur J Soil Sci 64:476–487
Hu Y, Li N, Jiang J, Xu Y, Luo X, Cao J (2021) Simultaneous Feammox and anammox process facilitated by activated carbon as an electron shuttle for autotrophic biological nitrogen removal. Front Environ Sci Eng 16:90
Hui C, Liu B, Du L, Xu L, Zhao Y, Shen D, Long Y (2022) Transformation of sulfidized nanoscale zero-valent iron particles and its effects on microbial communities in soil ecosystems. Environ Pollut 306:119363
Kampik C, Denis Y, Pagès S, Perret S, Tardif C, Fierobe HP, de Philip P (2020) A novel two-component system, XygS/XygR, positively regulates xyloglucan degradation, import, and catabolism in *Ruminiclostridium cellulolyticum*. Appl Environ Microbiol 86:01357–11320
Ke Y, Si S, Zhang Z, Geng P, Shen Y, Wang J, Zhu X (2023) Synergistic passivation performance of cadmium pollution by biochar combined with sulfate reducing bacteria. Environ Technol Innov 32:103356
Kong F, Wang J, Hou W, Cui Y, Yu L, Zhang Y, Wang S (2023a) Influence of modified biochar supported sulfidation of nano-zero-valent-iron (S-nZVI/BC) on nitrate removal and greenhouse gas emission in constructed wetland. J Environ Sci 125:568–581
Kong F, Ying Y, Lu S (2023b) Heavy metal pollution risk of desulfurized steel slag as a soil amendment in cycling use of solid wastes. J Environ Sci 127:349–360
Li T, Li W, Yu S, Zhao C, Liu L, Li YC, Gao B, Chen H, Wang B, Wang X, Wang S, Rinklebe J (2023) Biochar inhibited hydrogen radical-induced Cd bioavailability in a paddy soil. Sci Total Environ 892:164521
Liang L, Li X, Lin Z, Tian C, Guo Y (2020) The removal of Cd by sulfidated nanoscale zero-valent iron: the structural, chemical bonding evolution and the reaction kinetics. Chem Eng J 382:122933
Liao J, Hu A, Zhao Z, Liu X, Jiang C, Zhang Z (2021) Biochar with large specific surface area recruits $N_2O$-reducing microbes and mitigate $N_2O$ emission. Soil Biol Biochem 156:108212
Liu Q, Sheng Y, Wang W, Li C, Zhao G (2020) Remediation and its biological responses of Cd contaminated sediments using biochar and minerals with nanoscale zero-valent iron loading. Sci Total Environ 713:136650
Liu Q, Sheng Y, Wang W, Liu X (2021) Efficacy and microbial responses of biochar-nanoscale zero-valent during in-situ remediation of Cd-contaminated sediment. J Clean Prod 287:125076
Liu M, Wang J, Xu M, Tang S, Zhou J, Pan W, Ma Q, Wu L (2022) Nano zero-valent iron-induced changes in soil iron species and soil bacterial communities contribute to the fate of Cd. J Hazard Mater 424:127343
Liu N, Zhang Y, Zheng C, Tang C, Guan J, Guo Y (2023a) Sulfidated nanoscale zero valent iron for in situ immobilization of hexavalent chromium in soil and response of indigenous microbes. Chemosphere 344:140343
Liu S, Hao Y, Wang H, Zheng X, Yu X, Meng X, Qiu Y, Li S, Zheng T (2023b) Bidirectional potential effects of DON transformation in vadose zones on groundwater nitrate contamination: Different contributions to nitrification and denitrification. J Hazard Mater 448:130976
Loc NX, Tuyen PT, Mai LC, Phuong DT (2022) Chitosan-modified biochar and unmodified biochar for methyl orange: adsorption characteristics and mechanism exploration. Toxics 10:500
Lu HL, Li KW, Nkoh JN, Shi YXX, He X, Hong ZN, Xu RK (2022) Effects of the increases in soil pH and pH buffering capacity induced by crop residue biochars on available Cd contents in acidic paddy soils. Chemosphere 301:134674
Lyu C, Qin Y, Chen T, Zhao Z, Liu X (2022) Microbial induced carbonate precipitation contributes to the fates of Cd and Se in Cd-contaminated seleniferous soils. J Hazard Mater 423:126977
Ma Y, Zheng X, He S, Zhao M (2021) Nitrification, denitrification and anammox process coupled to iron redox in wetlands for domestic wastewater treatment. J Clean Prod 300:126953
Ma B, Shao S, Ai L, Chen S, Zhang L (2023) Influences of biochar with selenite on bacterial community in soil and Cd in peanut. Ecotoxicol Environ Saf 255:114742
Masuda Y, Shiratori Y, Ohba H, Ishida T, Takano R, Satoh S, Shen W, Gao N, Itoh H, Senoo K (2021) Enhancement of the nitrogen-fixing activity of paddy soils owing to iron application. Soil Sci Plant Nutr 67:243–247
Mitzia A, Vítková M, Ratié G, Chotěborský R, Vantelon D, Neaman A, Komárek M (2023) Revealing the long-term behaviour of nZVI and biochar in metal(loid)-contaminated soil: focus on Fe transformations. Environ Sci Nano 10:2861–2879
Muehe EM, Adaktylou IJ, Obst M, Zeitvogel F, Behrens S, Planer-Friedrich B, Kraemer U, Kappler A (2013) Organic carbon and reducing conditions lead to cadmium immobilization by secondary Fe mineral formation in a pH-neutral soil. Environ Sci Technol 47:13430–13439
Qi WY, Chen H, Wang Z, Xing SF, Song C, Yan Z, Wang SG (2023) Biochar-immobilized *Bacillus megaterium* enhances Cd immobilization in soil and promotes *Brassica chinensis* growth. J Hazard Mater 458:131921
Qu J, Yuan Y, Zhang X, Wang L, Tao Y, Jiang Z, Yu H, Dong M, Zhang Y (2022) Stabilization of lead and cadmium in soil by sulfur-iron functionalized biochar: performance, mechanisms and microbial community evolution. J Hazard Mater 425:127876
Rajendran M, Shi L, Wu C, Li W, An W, Liu Z, Xue S (2019) Effect of sulfur and sulfur-iron modified biochar on cadmium availability and transfer in the soil–rice system. Chemosphere 222:314–322
Shenk A, Ivan JPA, Schwede S, Odlare M (2022) Analysis of influencing characteristics of biochars for ammonium adsorption. Appl Sci 12:9487
Si S, Ke Y, Xue B, Zhang Z, Zhu X (2023) Immobilized sulfate reducing bacteria (SRB) enhanced passivation performance of biochar for Zn. Sci Total Environ 892:164556
Song B, Zeng G, Gong J, Liang J, Xu P, Liu Z, Zhang Y, Zhang C, Cheng M, Liu Y, Ye S, Yi H, Ren X (2017) Evaluation methods for assessing effectiveness of in situ remediation of soil and sediment contaminated with organic pollutants and heavy metals. Environ Int 105:43–55
Song H, Liang W, Luo K, Wang G, Li Q, Ji X, Wan J, Shao X, Gong K, Zhang W, Peng C (2023) Simultaneous stabilization of Pb, Cd, and As in soil by rhamnolipid coated sulfidated nano zero-valent iron: effects and mechanisms. J Hazard Mater 443:130259
Su Y, Adeleye AS, Keller AA, Huang Y, Dai C, Zhou X, Zhang Y (2015) Magnetic sulfide-modified nanoscale zerovalent iron (S-nZVI) for dissolved metal ion removal. Water Res 74:47–57
Su G, Chen B, Wu X, Xu J, Yang K, Lin D (2023) nZVI decreases $N_2O$ emission from pesticide-contaminated paddy soil. Sci Total Environ 892:164613

Sui L, Tang C, Cheng K, Yang F (2022) Biochar addition regulates soil phosphorus fractions and improves release of available phosphorus under freezing-thawing cycles. Sci Total Environ 848:157748
Teng Z, Zhao X, Jia B, Ye L, Tian S, Guo H, Guo Y, Ji X, Li T, Li M (2023) Bioremediation system consisted with *Leclercia adecarboxylata* and nZVI@Carbon/phosphate for lead immobilization: the passivation mechanisms of chemical reaction and biological metabolism in soil. J Environ Manag 340:117888
Tian H, Huang C, Wang P, Wei J, Li X, Zhang R, Ling D, Feng C, Liu H, Wang M, Liu Z (2023) Enhanced elimination of Cr(VI) from aqueous media by polyethyleneimine modified corn straw biochar supported sulfide nanoscale zero valent iron: performance and mechanism. Bioresour Technol 369:128452
Usman M, Zhao S, Jeon BH, Salama ES, Li X (2022) Microbial β-oxidation of synthetic long-chain fatty acids to improve lipid biomethanation. Water Res 213:118164
Wang Y, Liu Y, Su G, Yang K, Lin D (2021a) Transformation and implication of nanoparticulate zero valent iron in soils. J Hazard Mater 412:125207
Wang Y, Ren Q, Li T, Zhan W, Zheng K, Liu Y, Chen R (2021b) Influences of modified biochar on metal bioavailability, metal uptake by wheat seedlings (*Triticum aestivum* L.) and the soil bacterial community. Ecotoxicol Environ Saf 220:112370
Wang Y, Zheng K, Zhan W, Huang L, Liu Y, Li T, Yang Z, Liao Q, Chen R, Zhang C, Wang Z (2021c) Highly effective stabilization of Cd and Cu in two different soils and improvement of soil properties by multiple-modified biochar. Ecotoxicol Environ Saf 207:111294
Wang L, Wang Y, Li Y, Wang L, Zhu J, Zhang W, Zhang H, Niu L, Wu J (2022) Effect of water chemistry on nitrogen transformation, dissolved organic matter composition and microbial community structure in hyporheic zone sediment columns. Environ Res 215:114246
Wang Y, Jiang W, Tang Y, Liu Z, Qin Q, Xu Y (2023a) Biochar-supported sulfurized nanoscale zero-valent iron facilitates extensive dechlorination and rapid removal of 2,4,6-trichlorophenol in aqueous solution. Chemosphere 332:138835
Wang Y, Xie S, Zhou J, Fan G, He L, Fan X, Chen S, Yang J, Xu J, He Q (2023b) Sulfur cycle contributes to stable autotrophic denitrification and lower $N_2O$ accumulation in electrochemically integrated constructed wetlands: electron transfers patterns and metagenome insights. Chem Eng J 451:138658
Wang Z, Tan R, Gong J, Gong B, Guan Q, Mi X, Deng D, Liu X, Liu C, Deng C, Ding C, Zeng G (2023c) Process parameters and biological mechanism of efficient removal of Cd(II) ion from wastewater by a novel *Bacillus subtilis* TR1. Chemosphere 318:137958
Wang Z, Zhu S, Li S, Ma J, Zhang J, Gao P, Yan L (2023d) Unraveling the effects of the particle size on biomass properties, microbial community, and functional genes of denitrifying granular sludge. J Environ Chem Eng 11:109100
Wu Z, Firmin KA, Cheng M, Wu H, Si Y (2022) Biochar enhanced Cd and Pb immobilization by sulfate-reducing bacterium isolated from acid mine drainage environment. J Clean Prod 366:132823
Wu J, Hua Y, Feng Y, Xie W (2023a) Nitrated hydrochar reduce the Cd accumulation in rice and shift the microbial community in Cd contaminated soil. J Environ Manag 342:118135
Wu Z, Yang X, Huang L, Li S, Xia F, Qiu Y, Yi X, Jia P, Liao B, Liang J, Shu W, Li J (2023b) In situ enrichment of sulphate-reducing microbial communities with different carbon sources stimulating the acid mine drainage sediments. Sci Total Environ 898:165584
Xu C, Zhang K, Zhu W, Xiao J, Zhu C, Zhang N, Yu F, Li S, Zhu C, Tu Q, Chen X, Zhu J, Hu S, Koide RT, Firestone MK, Cheng L (2020) Large losses of ammonium-nitrogen from a rice ecosystem under elevated $CO_2$. Sci Adv 6:7433
Xu Y, Tang Y, Xu L, Wang Y, Liu Z, Qin Q (2021) Effects of iron-carbon materials on microbial-catalyzed reductive dechlorination of polychlorinated biphenyls in Taihu Lake sediment microcosms: enhanced chlorine removal, detoxification and shifts of microbial community. Sci Total Environ 792:148454
Xu M, Dai W, Zhao Z, Zheng J, Huang F, Mei C, Huang S, Liu C, Wang P, Xiao R (2022) Effect of rice straw biochar on three different levels of Cd-contaminated soils: Cd availability, soil properties, and microbial communities. Chemosphere 301:134551
Xu Y, Cao S, Chen X, Li J, Liu H, Gao Y, Wen S, Guo J, Shi X, Xue W (2023a) Enhanced immobilization of cadmium in contaminated paddy soil by biochar-supported sulfidized nanoscale zero-valent iron. J Soils Sediments 24(1):259–274
Xu Y, Meng X, Song Y, Lv X, Sun Y (2023b) Effects of different concentrations of butyrate on microbial community construction and metabolic pathways in anaerobic digestion. Bioresour Technol 377:128845
Xu Z, Liang W, Zhang X, Yang X, Zhou S, Li R, Syed A, Bahkali AH, Kumar Awasthi M, Zhang Z (2023c) Effects of magnesite on nitrogen conversion and bacterial community during pig manure composting. Bioresour Technol 384:129325
Xue W, Cao S, Zhu J, Li W, Li J, Huang D, Wang R, Gao Y (2022) Stabilization of cadmium in contaminated sediment based on a nanoremediation strategy: environmental impacts and mechanisms. Chemosphere 287:132363
Xue T, Liao X, Li H, Xie Y, Wei W, Chen J, Liu Z, Ji X (2023) Remediation of Cd contaminated paddy fields by intercropping of the high- and low-Cd-accumulating rice cultivars. Sci Total Environ 878:163133
Yan J, Qian L, Gao W, Chen Y, Ouyang D, Chen M (2017) Enhanced fenton-like degradation of trichloroethylene by hydrogen peroxide activated with nanoscale zero valent iron loaded on biochar. Sci Rep 7:43051
Yang X, Wen E, Ge C, El-Naggar A, Yu H, Wang S, Kwon EE, Song H, Shaheen SM, Wang H, Rinklebe J (2023) Iron-modified phosphorus- and silicon-based biochars exhibited various influences on arsenic, cadmium, and lead accumulation in rice and enzyme activities in a paddy soil. J Hazard Mater 443:130203
Yi Y, Wang X, Ma J, Ning P (2020) An efficient *Egeria najas*-derived biochar supported nZVI composite for Cr(VI) removal: characterization and mechanism investigation based on visual MINTEQ model. Environ Res 189:109912
Yin G, Chen X, Sarkar B, Bolan NS, Wei T, Zhou H, Wang H (2023) Co-adsorption mechanisms of Cd(II) and As(III) by an Fe-Mn binary oxide biochar in aqueous solution. Chem Eng J 466:143199
Yuan D, Wang G, Hu C, Zhou S, Clough TJ, Wrage-Mönnig N, Luo J, Qin S (2022) Electron shuttle potential of biochar promotes dissimilatory nitrate reduction to ammonium in paddy soil. Soil Biol Biochem 172:108760
Zhang W, Tan X, Gu Y, Liu S, Liu Y, Hu X, Li J, Zhou Y, Liu S, He Y (2020) Rice waste biochars produced at different pyrolysis temperatures for arsenic and cadmium abatement and detoxification in sediment. Chemosphere 250:126268
Zhang K, Zhang D, Wu X, Xue Y (2021a) Continuous and efficient immobilization of heavy metals by phosphate-mineralized bacterial consortium. J Hazard Mater 416:125800
Zhang Y, Ji H, Xi H, Zhu Y (2021b) Co-remediation of PTEs contaminated soil in mining area by heat modified sawdust and herb. Chemosphere 281:130908
Zhang C, Sun Y, Cao T, Wang W, Huo S, Liu Z-H (2022a) Influence of organic load on biogas production and response of microbial community in anaerobic digestion of food waste. Int J Hydrogen Energy 47:32849–32860
Zhang J, Yang X, Shi J, Zhao M, Yin W, Wang X, Wang S, Zhang C (2022b) Carbon matrix of biochar from biomass modeling components facilitates electron transfer from zero-valent iron to Cr(VI). Environ Sci Pollut Res 29:24309–24321
Zhang L, Wang Y, Hao S, Dou Q, Lan S, Peng Y (2022c) Anammox-synchronous zero-valent iron oxidation promoting synergistic nitrogen and phosphorus removal from wastewater. Biores Technol 347:126365
Zhang J, Jiang Y, Ding C, Wang S, Zhao C, Yin W, Wang B, Yang R, Wang X (2023a) Remediation of lead and cadmium co-contaminated mining soil by phosphate-functionalized biochar: performance, mechanism, and microbial response. Chemosphere 334:138938
Zhang J, Qian Y, Wang S, Yin W, Wang B, Yang R, Wang X (2023b) Effect and mechanism of biochar as a support on immobilization of different heavy metals by iron oxides in a multi-contaminated soil. J Environ Chem Eng 11:109895
Zhang J, Yang X, Wang S, Li T, Li W, Wang B, Yang R, Wang X, Rinklebe J (2023c) Immobilization of zinc and cadmium by biochar-based sulfidated nanoscale zero-valent iron in a co-contaminated soil: performance, mechanism, and microbial response. Sci Total Environ 902:165968
Zhang K, Yi Y, Fang Z (2023d) Remediation of cadmium or arsenic contaminated water and soil by modified biochar: a review. Chemosphere 311:136914

Zhang Q, Wang L, Xiao Y, Liu Q, Zhao F, Li X, Tang L, Liao X (2023e) Migration and transformation of Cd in four crop rotation systems and their potential for remediation of Cd-contaminated farmland in southern China. Sci Total Environ 885:163893
Zhang X, Li Q, Nie K, Cao K, Liao Q, Si M, Yang Z, Yang W (2023f) Synergistic effect of sulfidated nano zerovalent iron and proton-buffering montmorillonite in reductive immobilization of alkaline Cr(VI)-contaminated soil. Chemosphere 321:138132
Zhao Y, Li Q, Cui Q, Ni SQ (2022) Nitrogen recovery through fermentative dissimilatory nitrate reduction to ammonium (DNRA): carbon source comparison and metabolic pathway. Chem Eng J 441:135938
Zheng X, Wu Q, Huang C, Wang P, Cheng H, Sun C, Zhu J, Xu H, Ouyang K, Guo J, Liu Z (2023) Synergistic effect and mechanism of Cd(II) and As(III) adsorption by biochar supported sulfide nanoscale zero-valent iron. Environ Res 231:116080
Zhou Q, Liao B, Lin L, Qiu W, Song Z (2018) Adsorption of Cu(II) and Cd(II) from aqueous solutions by ferromanganese binary oxide–biochar composites. Sci Total Environ 615:115–122